Appl. Phys. B 62, 103–107 (1996)

Applied Physics B Lasers and Optics

Sound-velocity measurements in gases by laser-induced electrostrictive gratings

W. Hubschmid, R. Bombach, B. Hemmerling, A. Stampanoni-Panariello

Paul Scherrer Institut, CH-5232 Villigen PSI, Switzerland
(Fax: + 41-56/992199)

Received: 9 December 1994/Accepted: 7 February 1995

Abstract. Laser-induced electrostrictive gratings have been applied to measure the adiabatic sound velocity in various gases on a single-pulse basis. The gratings are generated by the interference of two parallel polarized, crossed excitation beams arising from a pulsed Nd: YAG laser at 532.1 nm, and are detected by diffracting a probe beam originating from a cw Ar^+ laser operating single-line at 514.5 nm. Measurements were performed in the overlap volume of unfocused and focused excitation beams. Using unfocused beams, the sound velocities in various gases at pressures of 5 bar were measured with a statistical error for single-pulse measurements of about 0.3%. With focused beams, the accuracy of the measurements is reduced because of the propagation of the sound waves out of the smaller overlap volume of 0.2 mm diameter and 4 mm length. Measurements with focused beams were performed in air and CO_2, with an error of about 1%.

PACS: 42.65.Es; 43.58. + z

Laser-induced gratings arise from the interference of two beams which intersect in a medium. The interference produces a spatially periodic light intensity distribution which may change the refractive index of the medium by various resonant or non-resonant mechanisms [1]. Electrostrictive gratings are generated at any frequency of the excitation beams. The dielectric medium is polarized by the electric field of the light waves. The spatial inhomogeneity of the electric field in the medium leads to a motion of mass towards regions of high laser intensity, eventually resulting in a sound wave [2]. In case of a non-vanishing thermal conductivity, also an isobaric density wave arises. The wavelength of the generated waves is defined by the fringe spacing of the interference pattern. The sound propagates into two opposite directions, normal to the planes of the fringes. The superposition of the counterpropagating sound waves and the isobaric density wave forms a spatial time-dependent grating.

Led by different intentions, various research groups recently studied the generation of laser-induced electrostrictive gratings in the gas phase [3–6]. The non-resonant signal contribution from an electrostrictive grating limits the sensitivity for the resonant signal in laser-induced grating spectroscopy [4]. It was shown in [4] that the temporal evolution of the signal is different for the resonant part and the electrostrictive contribution and therefore can be discriminated. Stampanoni et al. [5] investigated the electrostrictive grating formation for partially coherent excitation beams, demonstrating that it is strongly reduced by the application of incoherent excitation beams. On the other hand, the use of electrostrictive gratings has been proposed for diagnostic purposes. This has been illustrated by imaging a stream of helium in ambient air [3]. Cummings [6] and Stampanoni et al. [5] showed the possibility to use electrostrictive gratings to measure sound velocity (and therewith temperature) and acoustic attenuation in gases.

For the experiments described in this article, the gratings were excited by the frequency-doubled light of a pulsed Nd: YAG laser, and were observed by a cw Ar^+ laser (Sect. 1). A short account of the electrostrictive grating formation and of the determination of the sound velocity is given in Sect. 2. In Sect. 3, the results of the measurements of the adiabatic sound velocity for various gases are presented.

1 Experiment

The gratings are created by two excitation beams (EB1 and EB2) from a frequency-doubled Nd: YAG laser (Continuum, NY81-20) which intersect in a gas cell. The gratings are detected by diffracting a probe beam from a cw Ar^+ laser (Innova 70-4) operating single-line at 514.5 nm with a power of 1.7 W. The pulse length of the Nd: YAG laser is about 8 ns, its bandwidth is specified to be 1.0 cm^{-1} at 1064 nm, and its diameter is about 6 mm. For a maximal interaction, the difference in optical path length of the excitation beams is reduced to a small fraction of the pulse coherence length ($\approx$0.6 cm). This was

achieved by a variable delay line formed by two prisms in the path of EB2. Two different phase-matching geometries have been used for measurements with high and low spatial resolution, respectively. The arrangement, known as the nearly phase-conjugate geometry, is used for measurements with unfocused excitation beams resulting in a large overlap volume. The so-called 3-D forward phase-matching geometry is used with focused excitation beams.

In nearly phase-conjugate geometry (Fig. 1a), the two excitation beams (EB1, EB2) are produced by means of beam splitter BS1 ($R = 70\%$). The stronger beam, EB2, passes the delay line before it is directed by a 50% beam splitter BS2 into the gas cell where it crosses EB1 at an angle θ. With a beam diameter of 6 mm and a crossing angle $\theta = 3°$, the interaction volume has a length of about 13 cm. In the overlap volume, EB1 and EB2 have about equal intensity ($\approx 30\ \mathrm{MW/cm^2}$ each). The cw Ar^+ probe beam satisfies the Bragg condition and is diffracted from the grating into the signal beam. Employing the emission line of the Ar^+ laser at 514.5 nm, the signal beam and the probe beam are almost anticollinear to EB1 and EB2, respectively. Part of the signal passes through beam splitter BS2. The probe beam is perpendicularly polarized to the excitation beams. Stray light, mainly caused by beam splitter BS2, is efficiently reduced by a polarizer in the path of the signal beam.

In the 3-D forward-phase-matching geometry (Fig. 1b), beam splitter BS1 reflects 50% of the Nd: YAG output beam. EB2 passes the delay line. The two excitation beams and the probe beam are arranged parallel to each other in such a way that the excitation beams are lying on two neighboring corners of approximately a square and the probe beam on a third one. The three beams are crossed in the cell by focusing them through the same lens ($f = 400$ mm). In the focus the intensity of each of the excitation beams is about 3.5 $\mathrm{GW/cm^2}$. The signal leaving the sample passes through the fourth corner of the square and is collimated by a second lens ($f = 400$ mm). The measurement volume is approximately a cylinder of about 200 µm diameter ($1/e^2$ of the maximum intensity) and about 4 mm length. This geometry has the additional advantage that the whole signal can be collected and can easily be discriminated against scattered light by spatial filtering. Eventually, in both setups the signal is directed over a path of 5 m onto the aperture of a PhotoMultiplier Tube (PMT) (Philips XP2072). Stray light from the Nd: YAG laser is further suppressed by a notch filter (Kaiser Optical Systems) with a bandwidth of 9 nm at 532 nm in front of the PMT. The time-resolved acquisition of a single-pulse signal is performed by a digitizer (Tektronix, RTD720) with a full bandwidth of 500 MHz and a 2 GHz sampling rate. The data acquisition was accomplished by a personal computer.

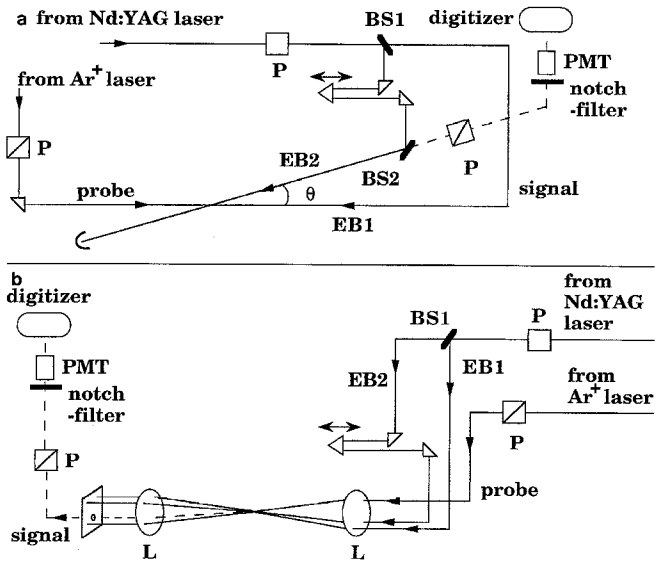

Fig. 1. **a** Experimental setup with nearly phase-conjugate geometry (*BS1*, Beam splitter ($R = 70\%$); *BS2*, Beam splitter ($R = 50\%$); *EB1, EB2*, Excitation beams; *P*, Polarizer; *PMT*, Photomultiplier tube). **b** Experimental setup with 3-D forward-phase-matching geometry (*BS1*, Beam splitter ($R = 50\%$); *EB1, EB2*, Excitation beams; *P*, Polarizer; *L*, Lens, focal length: 400 mm; *PMT*, Photomultiplier tube)

2 Theory

The reflectivity $R(t)$ of an electrostrictive grating is proportional to the square of the change in the refractive index, i.e., to the square of the change $\rho' = \rho - \rho_0$ of the medium density ρ from the homogeneous value ρ_0. The density change ρ' can be calculated by using the linearized equations of fluid dynamics with an electrostrictive-force term. Local thermal equilibrium is thereby assumed and also mutually coherent plane waves for the excitation beams. In an approximation which neglects thermal conductivity, the following equation can be derived [7]:

$$\frac{\partial^2 \rho'}{\partial t^2} - \Gamma' \Delta \frac{\partial \rho'}{\partial t} - v^2 \Delta \rho' = C \cos(qx)\, \delta(t - t_0). \tag{1}$$

Here, Γ' is a dissipation constant, depending on the viscosity, v is the adiabatic sound velocity of the medium, q is the modulus of the grating vector, Δ is the Laplacian, and C is a constant, indicating the strength of the excitation pulses. The excitation pulses were approximated by a δ-function at $t = t_0$; q is related to the fringe spacing: $q = 2\pi/\Lambda$. The fringe spacing Λ depends on the wavelength λ of the laser and on the intersection angle θ of the excitation beams according to $\Lambda = \lambda/[2 \sin(\theta/2)]$.

The spatial dependence in (1), being proportional to $\cos(qx)$, can be decoupled. The resulting equation of motion for $\rho'(t)$ is the equation of a damped harmonic oscillation. The solution is, in the case of weak (undercritical) damping:

$$\rho'(t) \propto \exp[-\beta(t - t_0)] \cos[\Omega(t - t_0)]. \tag{2}$$

The frequency Ω is related to the adiabatic sound velocity v in the medium. For small sound attenuation ($\beta \ll \Omega$), Ω is given by

$$\Omega = qv. \tag{3}$$

The attenuation constant β depends on Γ' according to $\beta = \Gamma' q^2/2$.

The reflectivity $R(t)$ of an electrostrictive grating, which is proportional to $[\rho'(t)]^2$, performs therefore an oscillation with a frequency 2Ω:

$$R(t) \propto \exp[-2\beta(t-t_0)]\{1-\cos[2\Omega(t-t_0)]\}. \quad (4)$$

If the thermal conductivity is taken into account in the fluid-dynamics equations, β will depend not only on the viscosity, but also on the thermal conductivity. Also, an oscillation of frequency Ω is superimposed to the 2Ω oscillation of (4). The Ω oscillation arises from the interference of the sound wave (Ω) with the isobaric density wave. The strength of the Ω oscillation is smaller than the 2Ω oscillation by a factor of the order β/Ω. Details on the solution of the full fluid-dynamics equations will be published in a forthcoming paper.

At low densities or high frequencies, which corresponds to strong sound attenuation, Ω is smaller than the value of (3). From the exact relation $\Omega(q)$, obtained by solving the full fluid-dynamical equations, one finds, e.g., for air at 1 bar and 26°C and a fringe spacing $\Lambda = 11.5$ μm, which are parameters of one of the experiments, a value $\Omega \approx 0.9995qv$. For Ar at 1 bar and 875°C, and $\Lambda = 11.5$ μm, one finds $\Omega \approx 0.992\, qv$. In the approximation where the Ω oscillation is neglected, relation $\Omega(q)$ can be written in the form [5]:

$$\Omega = qv[1 + (T_p/2\pi T)^2]^{-1/2}. \quad (5)$$

Here, $T_p = \pi/\Omega$ is the period and $T = (2\beta)^{-1}$ is the decay time of the grating by dissipation processes. This means that the difference of Ω from the value of (3) is small ($< 0.0015qv$), if three or more peaks of the grating oscillation are within the decay to a fraction 1/e of the initial reflectivity $R(t = t_0)$.

Published values of the sound velocity usually give the quantity v'. It is defined by the relation for the propagation of sound emitted by a source, say, at $x = 0$ [8]:

$$\rho'(x, t) = \exp(-\alpha x) \sin\left[\Omega\left(t - \frac{x}{v'}\right)\right]. \quad (6)$$

For small attenuation ($\alpha \ll \Omega/v'$), v' equals the adiabatic sound velocity v.

3 Results and discussion

The measurements were performed to determine the adiabatic sound velocity v. Thereby the quantity

$$v'' = \Lambda/2T_p, \quad (7)$$

which has the dimension of a velocity, was evaluated. In the range of the validity of (3), v'' is equal to v. In general, the correction factor by which v and v'' differ, as discussed after (4), was taken into account.

In the nearly phase-conjugate-beam geometry, the adiabatic sound velocity in Ar, N_2, and O_2 was measured at pressures of about 5 bar and room temperature. Figure 2 shows a measurement in O_2 at 5.55 bar and 26°C. The period T_p is 15.5 ns, corresponding to an acoustic frequency of 32.3 MHz. The imperfect modulation of the sine wave arises partially from the time response of the detection system, and partially from the divergence of the traveling sound waves building up the standing wave (see discussion below). The time response of the detection systems is given by the bandwidth of the digitizer (500 MHz) and the rise and decay time of the photomuliplier (≈3 ns each). The signal intensity peak-to-peak has fluctuations of about 10%. A computer simulation of the detection system taking into account the limited photon flux indicates that these fluctuations mostly arise from the photoelectron statistics at the cathode and the quantization noise of the digitizer. Measurements of the output energy of the Ar^+ laser in the frequency range of the oscillation frequencies around 60 MHz showed variations of less than 1%. The intensity fluctuations negligibly affect the accuracy of the measured T_p. The oscillation frequency and therewith T_p is determined by simply measuring the duration between some fixed number of oscillations of the grating. The largest error in the determination of the sound velocity arises from the geometric measurement of the angle θ. For the given beam diameter and a beam path of 1.5 m, as in the experiment, the error is about 1%. For our purposes, we performed a calibration measurement in argon with the value of the sound velocity taken from [9]. We thereby assume that dispersion can be neglected at the given frequency and pressure [10]. A value $\theta = 2.977 \pm 0.005°$ was obtained, corresponding to a grating spacing $\Lambda = 10.24$ μm. In Table 1, the sound velocities for O_2 and N_2 resulting from ten single-pulse measurements each are listed together with the obtained statistical errors. For comparison values for v' from [9] are given.

The interaction volume obtained from unfocused excitation beams, which intersect at a small angle, is quite large. For measurements in small samples or inhomogeneous media, it is desirable to have a better spatial resolution. This can be achieved by focusing the laser beams in a forward beam geometry (Fig. 1b). The two excitation beams, which are assumed to have a Gaussian spatial intensity distribution, are focused into the gas cell, where they interfere. The resulting spatial fringe pattern is sinusoidal with a Gaussian envelope having a waist spot size of about 200 μm. In this case, the effect of the propagation of the sound waves out of the small overlap volume is considerable. This results in a shorter lifetime of the

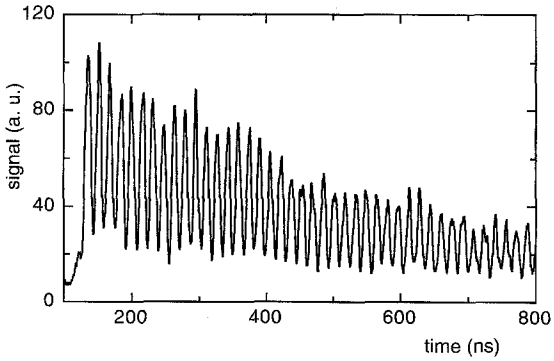

Fig. 2. Single-pulse measurement in O_2 at 5.55 bar and 26°C, performed with unfocused excitation beams in the nearly phase-conjugate geometry. The oscillation period of the grating reflectivity is 15.5 ns

Table 1. Single-pulse measurements of the adiabatic sound velocity v, given with statistical errors for single measurements. The setup used for the measurements is either U (with unfocused excitation beams) or F (with focused beams); f is the sound frequency of the performed measurement, v' are values of the sound velocity from [9, 10] at the frequencies f_{ref} and at the same conditions ϑ, p. For N_2, O_2, and air, dispersion at the given frequencies is small [10]

Gas	ϑ[°C]	p [bar]	Setup	v [ms^{-1}]	f [MHz]	v' [ms^{-1}]	f_{ref} [MHz]
N_2	25	5.53	U	352.4 ± 1.0	34.4	352.7 [9]	0
O_2	26	5.55	U	329.6 ± 0.6	32.3	329.5 [9]	0
Air	26.5	0.98	F	351.7 ± 2.3	30.7	347.1 [9]	0
CO_2	26.5	0.33	F	279.5 ± 2.6	24.4	280.3 [10]	0.6

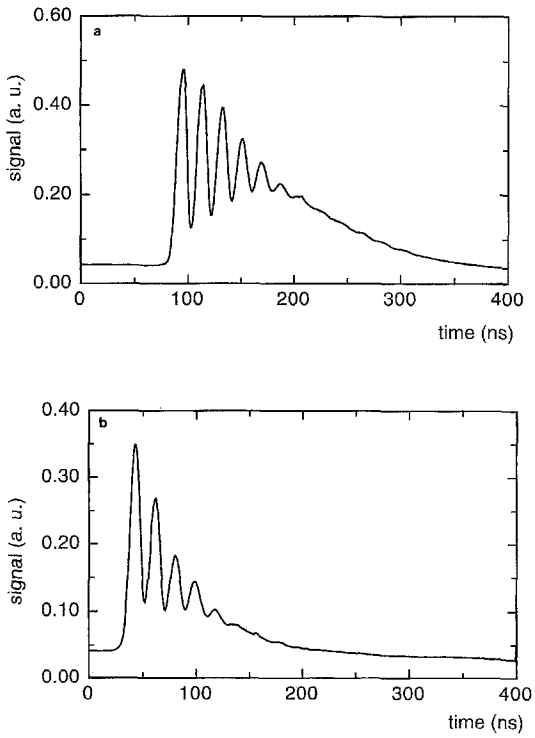

Fig. 3. a Measurement in Ar at 5 bar performed with focused excitation beams in the 3-D forward-phase-matching geometry. The signal intensity was averaged over 100 shots. The propagation of the sound velocity out of the beam overlap volume results in a non-oscillating, exponentially decaying contribution to the grating reflectivity. **b** Measurement in Ar at 1 bar. Otherwise, the experimental conditions and averaging were the same as in **a**. The effect of the propagation of the sound wave out of the beam overlap volume is less visible than in **a** because of the stronger dissipation of sound at 1 bar

standing acoustic wave, i.e., in a decrease of the number of the observable oscillations of the sound wave (peaks). The effect can especially be seen at high pressures, and it reduces the accuracy of the measured T_p and therewith of the sound velocity. Namely, the waves propagating out of the overlap volume give a contribution to the scattering reflectivity which is not oscillating but only decaying in time. The growth with time of this contribution leads to a reflectivity of the grating which is less and less modulated. The comparison of measurements in Ar at 5 bar (Fig. 3a) and Ar at 1 bar (Fig. 3b) illustrates this behaviour. In spite of a five-times smaller dissipation of the acoustic wave at 5 bar, compared to 1 bar, the number of visible peaks for both measurements is about the same. The non-oscillating part of the reflectivity, however, decays much slower at 5 bar.

The sound-velocity measurements with focused beams were performed with unattenuated beams of the Nd: YAG laser. To avoid optical breakdown in the gas, the pressure in the cell had to be kept below 1.5 bar. Single-pulse measurements were performed in Ar, CO_2, and air. The measurements in Ar were used, as before, to calibrate the angle θ. It was found to be $\theta = 2.660 \pm 0.005°$. This corresponds to a grating spacing $\Lambda = 11.46$ μm. An error of about 1% from dispersion between 0 and 30 MHz of the sound velocity in Ar at 1 bar may arise [10]. In Table 1, the results of the measurements are listed together with values from [9, 10]. Again, each value in the table is the average of ten measurements.

4 Conclusion

In summary, we showed that the adiabatic sound velocity in gases can be measured by a purely optical method using laser-induced electrostrictive gratings on a single-pulse basis. Being a non-resonant method, the excitation lasers do not have to be tuned to an absorption line of the medium. By changing the angle between the excitation beams, the possibility of a sound-velocity measurement in a large frequency range is given. In the experiments, the second harmonic of the output of a pulsed Nd: YAG laser was used for the excitation beams; the beam of a cw Ar^+ laser at 514.5 nm was used to read out the grating. The measurements with unfocused beams were performed in a nearly phase-conjugate geometry. Spatially resolved measurements with focused beams were performed in a 3-D forward-phase-matching geometry. The sound velocities at pressures of about 5 bar and room temperatures, measured with unfocused beams in N_2 and O_2 have been determined with a statistical error for single-pulse measurements of about 0.3%. Using focused beams, sound velocities in a cylinder of about 0.2 mm diameter and 4 mm length have been determined with an accuracy of about 1% at pressures of 1 bar or smaller pressures and room temperature.

Acknowledgement. We thank the Swiss Federal Office of Energy (BEW) for financial support.

References

1. H.J. Eichler, P. Günter, D.W. Pohl: *Laser-Induced Dynamic Gratings*, Springer Ser. Opt. Sci, Vol. 50 (Springer, Berlin, Heidelberg 1986) p. 38
2. K.A. Nelson, D.R. Lutz, M.D. Fayer, L. Madison: Phys. Rev. B **24**, 3261 (1981)
3. B. Hemmerling, A. Stampanoni-Panariello: Appl. Phys. B **57**, 281 (1993)
4. D.E. Govoni, J.A. Booze, A. Sinha, F.F. Crim: Chem. Phys. Lett. **216**, 525 (1993)
5. A. Stampanoni-Panariello, B. Hemmerling, W. Hubschmid: Phys. Rev. A **51**, 655 (1995)
6. E.P. Cummings: Opt. Lett. **19**, 1361 (1994)
7. R.W. Boyd: *Nonlinear Optics* (Academic, New York 1992) p. 334
8. K.F. Herzfeld, T.A. Litovitz: *Absorption and Dispersion of Ultrasonic Waves* (Academic, New York 1959) p. 39
9. *Encyclopédie des Gaz* (Elsevier, Amsterdam 1976)
10. Landolt-Börnstein: *Numerical Data and Functional Relationships in Science and Technology*, New Ser. II/5 (Springer, Berlin, Heidelberg 1967) pp. 127–137